Quantum Hall Effect from the Topological Surface States of Strained Bulk HgTe

C. Brüne,[1] C. X. Liu,[1] E. G. Novik,[1] E. M. Hankiewicz,[1] H. Buhmann,[1] Y. L. Chen,[2] X. L. Qi,[2] Z. X. Shen,[2] S. C. Zhang,[2] and L. W. Molenkamp[1]

[1]*Faculty for Physics and Astronomy and Röntgen Center for Complex Material Systems, Universität Würzburg, Am Hubland, D-97074, Würzburg, Germany*

[2]*Department of Physics, McCullough Building, Stanford University, Stanford, California 94305-4045, USA*

(Received 14 January 2011; revised manuscript received 18 February 2011; published 22 March 2011)

We report transport studies on a three-dimensional, 70-nm-thick HgTe layer, which is strained by epitaxial growth on a CdTe substrate. The strain induces a band gap in the otherwise semimetallic HgTe, which thus becomes a three-dimensional topological insulator. Contributions from residual bulk carriers to the transport properties of the gapped HgTe layer are negligible at mK temperatures. As a result, the sample exhibits a quantized Hall effect that results from the 2D single cone Dirac-like topological surface states.

DOI: 10.1103/PhysRevLett.106.126803 PACS numbers: 73.25.+i, 73.20.At, 73.43.−f

The discovery of two- (2D) and three-dimensional (3D) topological insulators (TIs) [1–10] has generated strong activity in the condensed matter physics community [11,12]. Current research on 3D TIs is mostly focused on Bi_2Te_3, Bi_2Se_3, and Sb_2Te_3 compounds [8–10] due to their simple Dirac-like surface states, which have been observed by angle-resolved photoemission spectroscopy (ARPES) and scanning tunneling microscopy [11]. However, these compounds show strong defect doping and low carrier mobility, and the observation of surface charge transport is obscured by the bulk conductivity. Many of the predicted novel properties of a 3D TI, such as the quantized magnetoelectric effect [13,14] and the surface Majorana fermions [15], can be observed only when bulk carriers are negligible compared to the surface states. Experimentally reaching the intrinsic TI regime, where bulk carriers are absent, is now the central focus of the field.

The two-dimensional TI state was first predicted and observed in 2D HgTe quantum wells [1,3], and nonlocal transport measurements demonstrate edge state transport without any contributions from 2D bulk carriers [16]. 3D HgTe is a semimetal which is charge-neutral when the Fermi energy is at the touching point between the light-hole and heavy-hole Γ_8 bands at the Brillouin zone center. A unique property of the band structure of HgTe is the energetic inversion of the Γ_6 and Γ_8 band ordering, which is the origin of the quantum spin Hall effect in 2D HgTe/CdTe quantum wells [3]. Because of the band inversion, 3D HgTe is also expected to have Dirac-like surface states [17,18], but since the material is semimetallic, this state is always coupled to metallic bulk states. With applied strain, a gap opens up between the light-hole and heavy-hole bands, so that strained 3D HgTe is expected to be a 3D TI [4,19]. In this Letter, we demonstrate experimentally that a gap opens up in in-plane strained 3D HgTe bulk layers grown by molecular beam epitaxy, and we reach the much sought after intrinsic TI regime in a material with negligible bulk carriers. In this regime, the Hall effect of the 3D HgTe bulk layer is quantized, due to the contributions from the surface states only. Theoretical considerations are in agreement with the experimental results and confirm the transport through 2D surface states with Dirac-type dispersion.

HgTe bulk samples have been grown by molecular beam epitaxy on CdTe substrates, which have a lattice constant that is 0.3% larger than that of bulk HgTe (0.646 nm). At this mismatch, the critical thickness for lattice relaxation is around 200 nm, implying that for thinner HgTe the epilayer adopts the lateral lattice constant of the substrate, while in thicker layers the strain is relaxed by the formation of dislocations.

To provide evidence for the occurrence of the topological surface state, we first show an ARPES measurement on a 1-μm-thick HgTe layer in Fig. 1(a). In this layer, the lattice strain is fully relaxed, and the surface has the lattice constant of unstrained bulk material. The figure clearly shows the presence of the predominantly linearly dispersing surface state band, coexisting with bulk bands (more data on these assignments can be found in Ref. [20]). According to the theoretical analysis in Ref. [19], the surface states originate from the inversion between the Γ_8 light-hole and Γ_6 electron bands, while the bulk bands, which appear nearly at the same energy range with the surface states, correspond to the Γ_8 heavy-hole band.

Since the relaxed sample is a semimetal and thus not a TI in the strict sense, we have grown a thinner sample, which is only 70 nm thick, thin enough for the epitaxial strain due to the lattice mismatch with the substrate to coherently strain the sample, thus opening up a bulk insulating gap. Figure 1(b) shows a high resolution x-ray diffraction map of the [115] reflex of this sample in units of reciprocal lattice space vectors. The bright spot in the center of this graph is the reflex from the substrate, while the thin vertical

 © 2011 American Physical Society

line stems from the HgTe epilayer. The absence of any relaxation of the reciprocal lattice vector $\mathbf{Q_x}$ for the epilayer is direct evidence that this sample is fully strained [21]. The deformation potentials of (Hg,Cd)Te have been reported in the literature [22]; using these values and the 0.3% lattice mismatch, we calculate an energy gap of the order of ~22 meV for fully strained HgTe on CdTe, using an eight-band $\mathbf{k} \cdot \mathbf{p}$ model [23]. We believe this energy gap to be the optimal gap value that can be obtained in HgTe. In principle, substrates with a larger lattice mismatch would induce a larger gap; however, these are not readily available. In addition, larger strain would also reduce the maximum thickness the HgTe layer can sustain without strain relaxation.

For transport experiments, we have subsequently patterned parts of both wafers into Hall-geometry devices with a mesa of 200 μm width and 600 μm length, using argon ion etching. The magnetotransport of the samples has been investigated at a base temperature of 50 mK, in magnetic fields up to 16 T. In the 1-μm-thick sample, the Hall data indicate that bulk conductance dominates the transport. Figure 1(c) shows that for this sample we observe a nonmonotonic dependence of the Hall voltage, which is characteristic for the multicarrier transport expected from a semimetal. Much more interesting behavior is observed for the 70-nm-thick sample, of which the longitudinal and Hall resistance are shown in the inset in Fig. 2. From the low field data, the electron mobility can be extracted and estimated as 34 000 $cm^2/(V \cdot s)$, which is significantly higher than that observed in Bi_2Se_3 and Bi_2Te_3 [24,25]. At high magnetic fields, the longitudinal and Hall resistance exhibit distinct features which are characteristic for a 2D electron system: The Hall resistance R_{xy} shows plateaus at the same magnetic fields where the longitudinal resistance R_{xx} develops a minimum (inset in Fig. 2). Additionally, the Hall resistance R_{xy} shows the expected 2D quantized plateau values, which become clearer in a conductivity plot (Fig. 2).

Compared with the quantum Hall effect of an ordinary 2D electron system, two unusual observations should be emphasized, which indicate that the observed quantum Hall plateaus indeed result from the Dirac-type dispersion of the topological surface states. First, at low magnetic fields, a sequence of Hall plateaus develops with odd filling factors $\nu = 9$, 7, and 5, before at higher field the sequence is continued with $\nu = 4$, 3, and 2. The occurrence of odd-number filling factors at low magnetic field indicates the presence of a zero mode (a Landau level at zero energy) due to the linear dispersion of Dirac fermions, as has also been found in graphene [26] and in HgTe/CdTe quantum wells with a critical thickness of 6.3 nm [27]. A 70-nm-thick layer can safely be regarded as a 3D material; the confinement energies of bulk carriers are sufficiently small that Hall quantization effects would be washed out by multisubband averaging. We thus assume that the Hall plateaus result from the topological surface states and use a model with two Dirac cones, one on the top (vacuum) and one on the bottom (CdTe interface) to describe the system

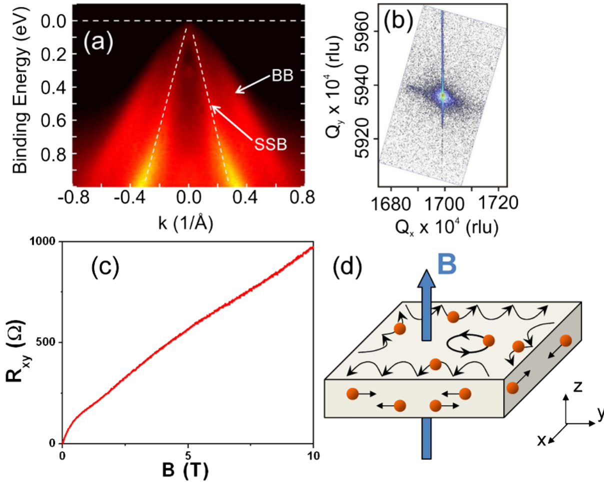

FIG. 1 (color online). Supporting characterization experiments. (a) ARPES measurements on a relaxed, 1-μm-thick HgTe sample. The dispersion of the surface state (SSB) and bulk bands (BB) are indicated by the arrows; (b) reciprocal space map in the region of the [115] reflex of the 70-nm-thick HgTe sample demonstrating that the epilayer is coherently strained; (c) Hall resistance as a function of the magnetic field of the semimetallic 1-μm-thick sample; (d) schematic picture of the coexistence of the chiral edge states from the upper and lower surfaces and the nonchiral metallic modes at the side surfaces. The magnetic field is perpendicular to the upper and lower surfaces but parallel to the four side surfaces.

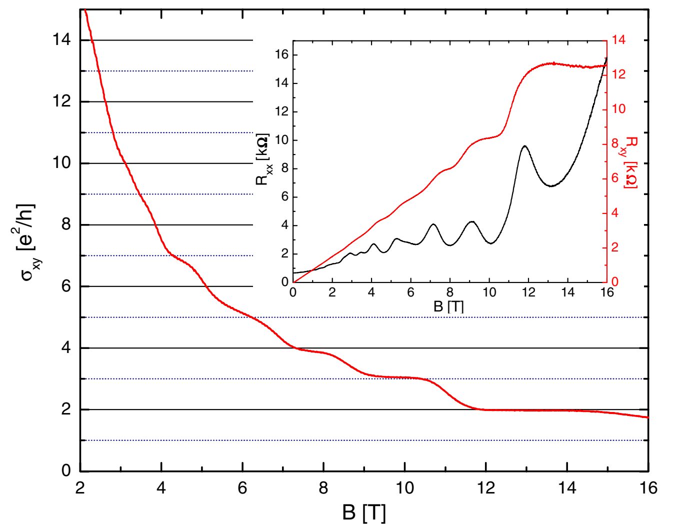

FIG. 2 (color online). Transport data on the strain-gapped 70-nm-thick HgTe sample. The Hall conductivity of the 70-nm-thick HgTe sample measured at 50 mK shows plateaus at the quantized values. The inset shows the Hall resistance R_{xy}, together with the longitudinal resistance R_{xx}.

(see Ref. [20] for details). Because massless Dirac fermions in a magnetic field always exhibit a zero mode, the Hall conductance of a single Dirac cone is given by $\sigma_{xy} = (n + \frac{1}{2})e^2/h$, where $n = n_t$ or $n = n_b$ (for the top and bottom surfaces, respectively) is always an integer [4,13]. The fractional factor of $\frac{1}{2}$ in the Hall conductance σ_{xy} is a consequence of the quantized bulk topological term in the electromagnetic action [13] and is independent of the microscopic details. When the top and the bottom surface have the same filling factor, i.e., $n = n_t = n_b$, the total Hall conductance is given by $\sigma_{xy}^T = (2n + 1)e^2/h$. Therefore, within the two Dirac cone model, the odd filling factor at low magnetic fields can be naturally explained by assuming both surfaces have the same density. The appearance of an even filling factor at high magnetic field indicates that the degeneracy is removed. In an ordinary 2D electron gas, such a lift of degeneracy usually occurs due to Zeeman coupling. However, Zeeman coupling cannot lift the degeneracy in inversion symmetric Dirac cones on the top and bottom surface of a topological insulator. As we explain in Ref. [20], this is because the inversion symmetry is preserved by the magnetic field. The Landau levels from the top and bottom surface states will remain degenerate as long as the hybridization between the two surface states is negligible. For a thickness of 70 nm, hybridization between the top and bottom surfaces can be neglected since the surface state width is around 2–3 nm. Thus we conclude that the inversion symmetry breaking is necessary for the explanation of the Landau level splitting. In practice, the different electrostatic environments of both surfaces break the inversion symmetry and lead to different densities at both surfaces. This then leads to different Landau filling factors for the top and bottom surfaces at high magnetic fields, and the visibility of even filling factors at high fields results from the increased energy splitting between adjacent Landau levels at lower filling factors in a Dirac system, as schematically indicated in the inset in Fig. 3. A calculation of the density of states in a magnetic field from a two Dirac cones model with an inversion breaking term indeed agrees well with the minima of the Shubnikov–de Haas oscillation, as shown in Fig. 3 (see Ref. [20] for details). From the fit, we obtain very reasonable carrier densities of 3.7×10^{11} cm^{-2} for the bottom (CdTe interface) and 4.8×10^{11} cm^{-2} for the top surfaces, respectively. We note that the carrier densities found here also imply that we can neglect any effects from bulk carriers—if the amount carriers found here were evenly distributed over the 70-nm slab, this would result in an overall 2D density of $\sim 10^{10}$ cm^{-2}, yielding a very different quantum Hall behavior.

The second observation is that the minima in R_{xx} do not approach zero even at the highest magnetic fields, although the Hall resistance is quantized and the plateaus have the expected resistance value. This indicates that, besides the chiral edge modes from the quantum Hall effect, there are other modes contributing to the longitudinal but not the Hall transport. A plausible candidate are the metallic states at the side surfaces [28]. While the above two Dirac cone model takes only the top and bottom surfaces explicitly into account, the topological surface states also occur on the four side surfaces, which see a parallel, rather than perpendicular, magnetic field. Consequently, at the side surfaces the Dirac points are not gapped but only shifted by the applied magnetic field. Thus, the surface states at the side surfaces will remain metallic in the magnetic field and coexist with the chiral edge states, as shown schematically in Fig. 1(d). This provides a backscattering mechanism when the transport on the top and bottom surfaces is in the quantum Hall regime [28]. A more systematic study of the influence of the residual bulk conductivity and side surface states is required to fully understand the quantitative behavior of R_{xx} and R_{xy}, which is beyond the scope of the present Letter.

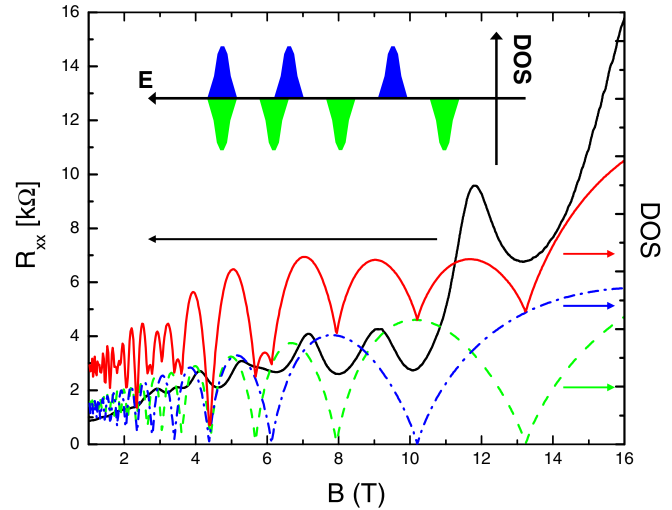

FIG. 3 (color online). Comparison between the calculated density of states (DOS) and the measured Shubnikov–de Haas oscillations. The DOS are calculated for a two Dirac cones model for the surface states with one Dirac cone (at the CdTe interface) having a carrier density 3.7×10^{11} cm^{-2} (blue dashed-dotted line) and the other (the surface facing vacuum) 4.8×10^{11} cm^{-2} (green dashed line). The sum of the DOS for the two Dirac cones (red line) compares well with the measured longitudinal resistance R_{xx} (black line). The inset shows the Landau ladders of the Dirac fermions on both surfaces.

In summary, we have experimentally reached the much sought after regime of the intrinsic 3D topological insulator with negligible bulk carriers, in an epitaxially strained 3D HgTe sample. Our observation of a quantized Hall conductance in a 3D sample conclusively demonstrates a key feature of 3D topological insulators. A simple model with two Dirac cones is proposed to understand the most salient features of the transport measurement qualitatively. The quality of our sample should be sufficient to observe the quantized topological magnetoelectric effect [13]

and directly determine the 3D topological invariant experimentally.

We acknowledge useful discussions with G. Astakhov, J. E. Moore, and A. H. MacDonald. This work was supported by the German Research Foundation DFG [SPP 1285 Halbleiter Spintronik, DFG-JST joint research program, and Grants No. AS327/2 (E. G. N.) and No. HA5893/1-1 (E. M. H.)], the Alexander von Humboldt Foundation (C. X. L. and S. C. Z.), the EU ERC-AG program (L. W. M.), and the U.S. Department of Energy, Office of Basic Energy Sciences, Division of Materials Sciences and Engineering, under Contract No. DE-AC02-76SF00515 (S. C. Z., Z. X. S., and Y. L. C.).

[1] B. A. Bernevig, T. L. Hughes, and S. C. Zhang, Science **314**, 1757 (2006).
[2] C. L. Kane and E. J. Mele, Phys. Rev. Lett. **95**, 226801 (2005).
[3] M. König, S. Wiedmann, C. Brüne, A. Roth, H. Buhmann, L. Molenkamp, X.-L. Qi, and S.-C. Zhang, Science **318**, 766 (2007).
[4] L. Fu and C. L. Kane, Phys. Rev. B **76**, 045302 (2007).
[5] L. Fu, C. L. Kane, and E. J. Mele, Phys. Rev. Lett. **98**, 106803 (2007).
[6] J. E. Moore and L. Balents, Phys. Rev. B **75**, 121306 (2007).
[7] D. Hsieh, D. Qian, L. Wray, Y. Xia, Y. S. Hor, R. J. Cava, and M. Z. Hasan, Nature (London) **452**, 970 (2008).
[8] H. Zhang, C.-X. Liu, X.-L. Qi, X. Dai, Z. Fang, and S.-C. Zhang, Nature Phys. **5**, 438 (2009).
[9] Y. Xia, D. Qian, D. Hsieh, L. Wray, A. Pal, H. Lin, A. Bansil, D. Grauer, Y. Hor, R. Cava, and M. Z. Hasan, Nature Phys. **5**, 398 (2009).
[10] Y. L. Chen *et al.*, Science **325**, 178 (2009).
[11] M. Z. Hasan and C. L. Kane, Rev. Mod. Phys. **82**, 3045 (2010).
[12] J. E. Moore, Nature (London) **464**, 194 (2010).
[13] X.-L. Qi, T. L. Hughes, and S.-C. Zhang, Phys. Rev. B **78**, 195424 (2008).
[14] A. M. Essin, J. E. Moore, and D. Vanderbilt, Phys. Rev. Lett. **102**, 146805 (2009).
[15] L. Fu and C. L. Kane, Phys. Rev. Lett. **100**, 096407 (2008).
[16] A. Roth, C. Brüne, H. Buhmann, L. W. Molenkamp, J. Maciejko, X.-L. Qi, and S.-C. Zhang, Science **325**, 294 (2009).
[17] Y. C. Chang, J. N. Schulman, G. Bastard, Y. Guldner, and M. Voos, Phys. Rev. B **31**, 2557 (1985).
[18] O. A. Pankratov, Semicond. Sci. Technol. **5**, S204 (1990).
[19] X. Dai, T. L. Hughes, X.-L. Qi, Z. Fang, and S.-C. Zhang, Phys. Rev. B **77**, 125319 (2008).
[20] See supplemental material at http://link.aps.org/supplemental/10.1103/PhysRevLett.106.126803 for details on the ARPES experiments and theoretical models.
[21] G. Bauer and W. Richter, *Optical Characterization of Epitaxial Semiconductor Layers* (Springer, Berlin, 1996), Chap. 6, pp. 287–391.
[22] S. Adachi, *Properties of Semiconductor Alloys: Group-IV, III-V and II-VI Semiconductors* (Wiley, New York, 2009).
[23] E. G. Novik, A. Pfeuffer-Jeschke, T. Jungwirth, V. Latussek, C. R. Becker, G. Landwehr, H. Buhmann, and L. W. Molenkamp, Phys. Rev. B **72**, 035321 (2005).
[24] J. G. Analytis, R. D. McDonald, S. C. Riggs, J. Chu, G. S. Boebinger, and I. R. Fisher, Nature Phys. **6**, 960 (2010).
[25] D. Qu, Y. S. Hor, J. Xiong, R. J. Cava, and N. P. Ong, Science **329**, 821 (2010).
[26] A. H. Castro Neto, F. Guinea, N. M. R. Peres, K. S. Novoselov, and A. K. Geim, Rev. Mod. Phys. **81**, 109 (2009).
[27] B. Buettner, C. Liu, G. Tkachov, E. Novik, C. Bruene, H. Buhmann, E. Hankiewicz, P. Recher, B. Trauzettel, S. Zhang, L. W. Molenkamp, Nature Phys. (in press).
[28] R. Chu, J. Shi, and S. Shen, arXiv:1007.0497.